Estimating Riparian Vegetation Geometry and Biomass from LiDAR Point Clouds

Proceedings of the 39th IAHR World Congress
19-24 June 2022
Granada, Spain
DOI number

Estimating Riparian Vegetation Geometry and Biomass from LiDAR Point Clouds

Melissa Latella[(1)], Tommaso Raimondo[(1)] and Carlo Camporeale[(1)]

[(1)]Department of Environment, Land and Infrastructure Engineering, Politecnico di Torino, Torino, Italy,
melissa.latella@polito.it

Abstract

In non-arid environments, the evolution of rivers and floodplains is an eco-morphodynamic process conditioned by riparian vegetation dynamics and continuous feedback among plants, water, and sediments. Because of these mutual interactions, proper quantification of vegetation geometry and biomass in riparian corridors is needed to carry out realistic eco-morphodynamic fluvial modeling and support the management of riverine ecosystems. The use of remote sensing in river sciences has notably increased in recent years, emphasizing the application of Light Detection And Ranging (LiDAR) at different scales, from single fluvial bars up to river reaches. Nevertheless, despite forestry having a long experience in LiDAR-based vegetation inventory, the transfer of knowledge to eco-morphodynamic applications still needs to be addressed appropriately. The present work aims to explain why LiDAR has started to be employed for vegetation inventory and how it may support eco-morphodynamic modeling. After introducing the different approaches to performing plant inventory with LiDAR point clouds, we present two methodologies that we have recently defined to map and measure individual trees and shrubs along rivers and highlight their strengths and weaknesses. These methods integrate targeted field measurements with LiDAR datasets and can be combined in a single innovative procedure. By referring to the Orco River case in northwest Italy, we show the procedure applications, opening up for discussion about future developments in this direction.

Keywords: LiDAR; Point clouds; Riparian vegetation; Field measurements; River modelling

1. INTRODUCTION

Plants actively influence fluvial and riparian landscape evolution. Wherever environmental conditions allow vegetation to settle, plants interact with water and sediments, affecting water flow and sediment patterns while being subjected to flooding, burial, uprooting, and the variability of nutrients and soil moisture. Eco-morphodynamics attempts to investigate these processes through field observations and models. Regarding the latter, the literature offers a miscellaneous collection. Several analytical eco-morphodynamic models have been defined since the 2000s (Vesipa et al., 2017), mainly focusing on the time-evolution of vegetation biomass in response to hydrological and topographical forcing. The development of numerical models in this direction is relatively recent and still at its early stage. Some software accounts for the additional flow resistance due to plants if a map of vegetation features and a law to compute the roughness coefficients are provided (e.g., Järvelä, 2004). A few works have also encompassed the feedback between vegetation and morphodynamics by coupling the underlying algorithm with other modules accounting for vegetation dynamics (van Oorschot et al., 2016; Kleinhans et al., 2018).

Generally, the works mentioned above focus on ideal or almost-real rivers since translating them into quantitative eco-morphodynamic tools would require an effort to estimate vegetation biomass (for analytical models) and geometry (for numerical models) and provide maps of these estimates. Field surveys alone (traditionally the data source of vegetation features) are insufficient for this task.

To address the need for quantitative, spatially continuous data, remote sensing (RS) has started to replace or accompany field surveys in the last decades. The use of RS to support river and riparian sciences has recently widened by addressing the characterization of vegetation, sediments, and water resources at various spatial scales. RS is generally more cost-effective than field activities, enabling the coverage of larger areas. Nevertheless, the extent of RS advantage rather than field activities strongly depends on the chosen technique, and it demands computational effort and the knowledge or development of proper tools for data analysis.

The present work explores the possibility of integrating field data with RS to support eco-morphodynamic modeling. For this purpose, it reviews the recent efforts made in this direction by Latella et al. (2021) and the following research. The remainder of the manuscript is organized as follows: Section 2 explains the choice of a particular RS technique -- called Light Detection and Ranging (LiDAR) -- for riparian studies, the different ways to perform vegetation inventory based on LiDAR data, and the methods to deal with biomass and geometry

estimation of mature trees and shrubs, respectively; Section 3 presents a case study reporting some examples of the outcomes deriving from the two described methods; Section 4 further discusses some crucial aspects of the presented approaches. The final purpose is to provide an overall picture of the developed tools and point out the remaining open issues, hoping to stimulate a broader discussion about the potential application of LiDAR data for riparian modeling and management.

2. METHODS

2.1 Selecting the remote sensing technique

Despite the large variety of available RS data and tools, we focused on Light Detection and Ranging (LiDAR) mounted on airborne laser scanners (ALS). A good compromise between the areal extent and spatial resolution this technology offers drove this choice. For instance, satellite imagery may cover up to the global scale, but the freely available datasets generally have a coarse resolution. On the contrary, terrestrial laser scanners yield very high-resolution data but cover circumscribed areas. Moreover, due to governmental monitoring plans, LiDAR data coverage is rapidly increasing at the regional/national scale.

LiDAR returns spatial distances by computing the elapsed time between the emission of an electromagnetic signal and its reception after reflection from a target surface. LiDAR datasets generally consist of a georeferenced point cloud describing the ground and all the objects standing on it. LiDAR sensors are labeled as *red* or *green* depending on the wavelength of their emitted signals and the capability of penetrating water. Red LiDARs are cheaper and more common, albeit entirely absorbed by water. In our research, we used red LiDARs since their limitations do not hamper riparian vegetation mapping, which was our primary goal.

Historically, LiDAR has been exploited extensively in forestry. Its potential in this field is related to the partial reflection of the electromagnetic signal from plants, resulting in the three-dimensional description of the forest structures, which, instead, is not provided by most of the other RS techniques. However, the knowledge transfer from forestry to river sciences is still in its infancy. Although the use of LiDAR for riparian vegetation studies has steadily increased since the 2000s (Carbonneau and Piégay, 2012; Huylenbroeck et al., 2020; Piegay et al., 2020), only a few works have addressed vegetation mapping (e.g., Latella et al., 2021), biomass estimation (Cartisano et al., 2013; Latella et al., 2020; Huylenbroeck et al., 2021) and roughness definition (e.g., Straatsma and Baptist, 2008).

2.2 Forest inventory approaches

Forest inventory from LiDAR data can be carried out through two opposing approaches, namely the *area-based* and *individual tree-based* methods (Yu et al., 2010), both generating accurate results when calibrated with ground data (Duncanson and Dubayah, 2018).

The *area-based* approach generally yields vegetation features averaged at the stand level, such as the basal area, overall volume and biomass, and the mean canopy height. Such information is retrieved from regressions between LiDAR height percentiles and field data. In the case of riparian applications, we found the area-based method helpful whenever low-density LiDAR datasets (i.e., resolution of 2 points$\times$m^{-2} or less) are available. To the best of our knowledge, Latella et al. (2020) were the first to use this to calibrate an eco-morphodynamic model for riparian corridors after estimating vegetation biomass. Relying on low-density datasets and an area-based approach, they provide the approximated riparian biomass distribution and averaged vegetated features in a relatively fast and little demanding way, needing little computational effort and some field measurements. Nevertheless, this method also shows some limitations: (i) the low point density forces the use of two-dimensional LiDAR products (e.g., the canopy height model, CHM) not leveraging the three-dimensionality of the point cloud; (ii) no information about the stem density (i.e., number of stems per unit area) can be obtained; (iii) the CHM does not describe understory vegetation and (iv) juvenile plants are hardly detected if the dataset has a coarse resolution. In light of these considerations, we may state that the range of eco-morphodynamic applications remains limited, suitable for simple analytical models that require overall biomass as input, such as in Latella et al. (2020) or similar works (e.g., Muneepeerakul et al., 2007; Perona et al., 2009).

As mentioned above, advanced numerical eco-morphodynamic models require information at the individual plant level. For instance, the definition of a roughness map relies on the knowledge of stem density and plant geometry, while the setting computational routine accounting for vegetation dynamics relies on vegetation arrangement at a specific time. The second approach, defined as *individual tree-based*, might address these needs by collecting information for each plant and deriving the other attributes through calibrated allometric models. The following two sections describe the latest developments of tree and shrub mapping based on this approach.

2.3 Method 1: dealing with mature trees

After detecting the individual trees within a given area, individual tree-based inventories provide, among others, the stem density, which is a crucial variable for eco-morphodynamic models. By examining the literature, we found out that most of the methods for individual tree detection (ITD or individual crown detection ITC) work similarly by interpolating the first returns of the LiDAR clouds into a canopy height model (CHM) and labeling the peaks of the interpolated surface as individual trees. The accuracy of these methods largely depends on the grid size of the CHM since coarse grids are associated with excessive peak smoothing, whereas too fine grids are affected by noise. In addition, tree species strongly impact detection accuracy. Most of these models have been developed for coniferous forests, favored by the conical shape of trees and the reduced presence of understory vegetation. However, they are less suitable for applications along rivers in temperate climates where vegetation mostly belongs to deciduous species. Indeed, the rounded and overlapping crowns of deciduous trees prevent the formation of univocal peaks in the CHM, and the local height maxima might not correspond to individuals.

Latella et al. (2021) proposed a new algorithm leveraging the full three-dimensionality of LiDAR datasets to overcome this limitation. Although other works have attempted to leave behind the CHM interpolation, this algorithm innovatively relies on the assumption that the point cloud becomes denser in correspondence with the tree center. This assumption has found confirmations both in the literature (Rahman and Gorte, 2008) and in data visualization. We here shortly describe the workflow, but more details can be found in the original work. Firstly, the algorithm applies filters to remove outliers and points associated with grasses and bushes from the input cloud. Secondly, it moves from space to frequency domain to find the optimal size of the neighborhood for each point. It uses the optimal neighborhood size to compute the areal point density, whose local maxima represent individual stems. Thirdly, it similarly determines the typical spacing among trees and removes all those stems too close to one another. Finally, it detects the treetops as the highest closest points with respect to the identified stems and eventually removes anthropic objects.

The method achieves high performance both in plantations and wild stands. Recall, precision, and F-score metrics are always higher than 70% for points clouds having at least 2 points$\times m^{-2}$, and the position error is generally comparable with the precision of the measuring instrumentation. It has dealt with understory vegetation, unlike the CHM-based ones. Moreover, it is expected to perform well also in coniferous trees because of its underlying assumption. It has already shown high accuracy when applied to non-LiDAR clouds, such as photogrammetric ones, especially with multi-temporal datasets (Belcore and Latella, under review), therefore offering a broader range of applications than CHM-based methods. Furthermore, the method is highly versatile. For instance, the algorithm generates tree geometry maps, or it can be coupled with a procedure to associate the tree features with mesh nodes and provide all the input required by hydrodynamic models for roughness computation.

Despite the numerous potentialities, the method also has some weaknesses to consider for proper usage. We remark that the higher the nominal point density, the higher the accuracy and the computational time, making it less competitive wherever CHM-based methods, which are generally quite fast, perform well. Finally, working on the whole cloud also translates into a need for parallelization when applied to large clouds requiring a partition of the study site in the case of large datasets before its application.

2.4 Method 2: including shrubs and bushes

The high disturbance associated with hydrological fluctuations and flooding causes a periodical rejuvenation of vegetation in riparian areas. The biomass of young trees and bushes is generally not concentrated in a stem but more homogenously distributed within the plant volume. Shrubs and bushes may have high stem density, or their biomass may be mainly composed of foliage and thin branches. Furthermore, often these plants are not arranged as isolated individuals but clustered. These features are not consistent with the underlying assumption of the algorithm presented in Section 2.3 (i.e., increasing point density towards the plant center), whose application is, therefore, suitable for adult trees only.

To address the criticalities above, inventory based on LiDAR datasets should work directly on the plant geometry and be flexible enough to consider isolated individuals and clusters. To the best of our knowledge, we were the first to propose a solution in this direction so far. We adapted and merged different literature methods to define a strategy to retrieve the height, cross-sectional area, and volume of an individual plant by iteratively working on slices of the input point cloud. Later, we embedded this method in a broader procedure to apply biomass estimation to extended areas, such as a river reach. The new procedure generates a shrub mask by processing RGB imagery and excluding the mature trees identified by the method explained in Section 2.3. Subsequently, the procedure detects the individuals and the clusters from the shrub mask, clips the input point cloud according to them, and applies the method to retrieve the plant (or cluster) geometry. Finally, it carries

out biomass budget and representation over maps by using the biomass bulk density deriving from our field measurements.

The procedure supports automated biomass and carbon budgets over extended areas requiring targeted field observations. Despite its computational effort, it allows overcoming the labor demanded by extensive field surveys and visual inspection of remote sensing imagery, resulting in more cost-effective and spatially continuous information to be used in eco-morphodynamic modeling.

Also in this case, weaknesses must be acknowledged. We applied the procedure to a high-resolution point cloud (9 points$\times$m^{-2}), but the leaf-off conditions of our dataset may have hampered the geometrical reconstruction of the smallest plants. Moreover, we had to measure biomass bulk density consistently with the reconstruction of LiDAR-derived geometries since the literature does not provide this kind of information. Therefore, the range of applicability of the procedure depends on the possibility of retrieving (from literature or in the field) bulk density values to convert the estimated volumes in biomass and acquisition conditions. These latter mainly consist of the nominal point density, since the fewer the points representing a shrub, the worst the plant geometrical reconstruction and the presence of foliage, preferring leaf-on conditions.

3. CASE STUDY

3.1 The Orco River site

We here provide an example of the presented methodologies by referring to the measurements and data analysis carried out in the Orco River active channels and floodplain in northwest Italy. The Orco River is a wandering gravel-bed river characterized by an alpine and high energy behavior. It is approximately 90 km long and has a catchment area of 930 km^2, springing from the Gran Paradiso massif and ending at the confluence with the Po River nearby the town of Chivasso. The study site is centered at N 45°14' 22" - E 7°48' 45" and stretches for more than 30 km from the town of Cuorgné until the confluence with the Po River (Figure 1 A-B).

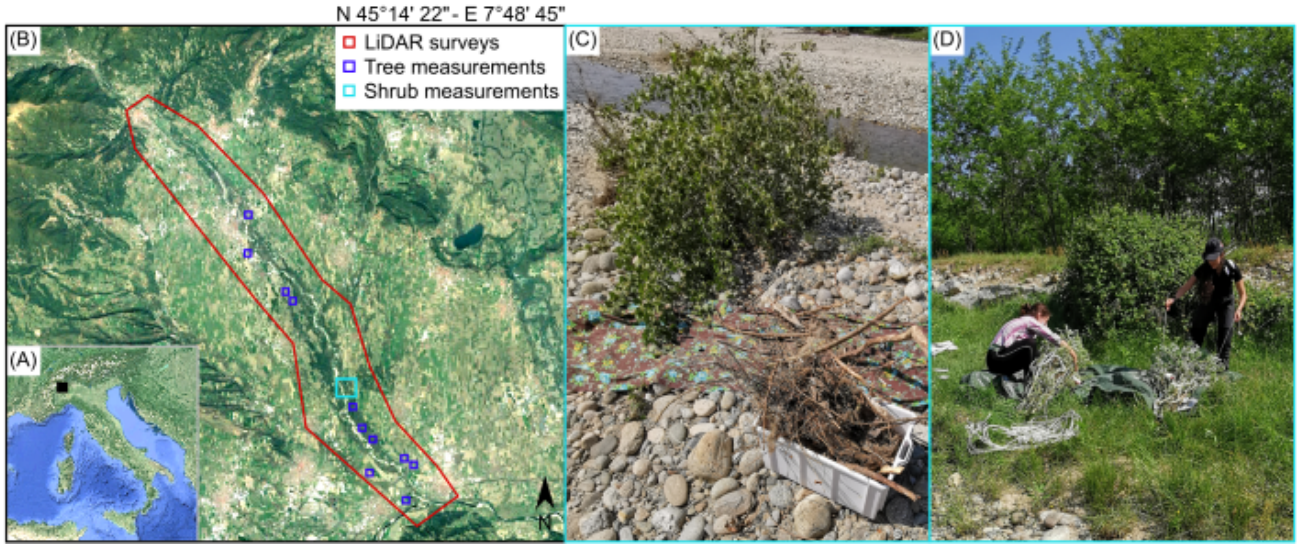

Figure 1. The study site is located in northwest Italy (A) and comprises a reach of the Orco River (B) that have been surveyed through LiDAR and field measurements, such as plant volume and weight estimation (C-D).

Human presence in the Orco River floodplain is mainly related to silviculture, farming, damming, and mining. However, the river still exhibits highly dynamic behavior with a moderate annual migration rate (approximately 10 m$\times$yr^{-1}). The floodplain is generally flat or very gentle, except close to the riverbanks. The mean bed slope is 0.5%, and D_{50} is 0.075 m.

Bearing coarse sediments are found within and close to the active channel(s), despite being rarely substituted by sand deposits colonized by herbaceous species. Juvenile deciduous individuals of aspens (*Populus tremula* L., *Populus alba* L., *Populus nigra* L.) and willows (*Salix alba* L., *Salix purpurea* L.), periodically disturbed by flooding, colonize the river bars. Moving inland, mature willows and aspens stand in the floodplain, together with old black locusts (*Robinia pseudoacacia* L.), European oaks (*Quercus robur* L.), and hornbeams (*Carpinus betulus* L.). Some forest stands belong to commercial plantations with trees of the same cohorts arranged according to regular patterns. However, wild patches of trees of different sizes and ages with overlapping crowns and understory vegetation occupy most of the area.

3.2 Airborne laser scanner data

The Italian National Council of Research – Research Institute for Geo-Hydrological Protection (CNR-IRPI) of Torino carried out two airborne laser scanner (ALS) LiDAR campaigns on 28 February 2019 and 23 March 2021.

CNR-IRPI designed the two surveys to be potentially identical in equipment setup, covered areas, achieved resolution, and environmental conditions. They used a LiteMapper 6800 installed on a POD DART and guaranteed a raw coverage equal to 9 points$\times$m^{-2}. Being winter, both the surveys were carried out in leaf-off conditions. The campaigns yield georeferenced point clouds and RGB orthophotos with a pixel resolution of 0.07 m. Further details can be found in Latella et al. (2021).

3.3 Field measurements

During the first LiDAR campaign, we performed tree inventory for random stands within the study area. We recorded the tree position employing a Real-Time Kinematic Global Positioning System (RTK-GPS), model ROVER LEICA 1250, and GNSS smart antenna. The position error was approximately 1.0 m because of the reduced signal, requiring a cross-check with a visual inspection of the companion orthophotos of the LiDAR point clouds. The inventory also comprised measurements of the tree height through a laser rangefinder (Trupulse 360R, Laser Technology, Centennial, Colorado, USA) and diameter at breast height (DBH)[1] with measuring tape of 0.001 m precision. These measurements allowed us to regress allometric relationships to determine tree volume whenever either the height or the DBH is known.

In addition, we came back into the field on 27 May 2021 to perform an inventory of eighteen selected shrubs belonging to the two most common species found on Orco river bars, ten aspens (*Populus tremula* L.) and eight white willows (*Salix alba* L.). We measured tree height (graduated rods with 0.01 m precision) and cross-sectional area (measuring tape with 0.001 m precision) according to a repeatable and straightforward procedure to compute the overall plant volume (Figure 1 C-D). After cutting, we weighted each individual with a portable scale (0.001 kg precision) to determine the aboveground biomass and the biomass bulk density.

3.4 Methodology outcomes

Figure 2 shows an example of the methodology's outcome for a subset of the study site. By dealing separately with trees and shrubs, the procedure can generate a map of the areal biomass within the investigated area. In this example, the comparison between the biomass maps for 2019 and 2021 and the associated biomass budgets allowed us to understand the vegetation dynamics that occurred in the considered period. Part of the biomass disappeared because of fluvial processes, such as erosion and flooding. Some trees were instead removed to leave space for dirt roads. However, vegetation growth also occurred in the less disturbed zones, partially outbalancing the biomass loss. The biomass budget further confirms this fact by indicating a rise in the overall biomass from 508.9±29.8 Mg to 621.6±44.3 Mg. The analysis may also be refined by considering trees and shrubs separately. In this case, we observe a rise of 28.4% and 19.8% for tree biomass and occupied area, respectively, while we see a biomass increment of 6.8% for shrub biomass associated with a dramatic reduction of the occupied area equal to 31.6%. These budgets, coupled with map visualization, clearly indicate that the enlargement of tree crowns and the growth of individuals identified as shrubs in 2019 and trees in 2021 outbalanced the tree removal due to dirt roads. They also highlight the dramatic influence of river processes to shrub biomass loss, although this was utterly compensated and exceeded by the plant growth. This behavior is typical of riparian pioneer species, whose fast growth rate, especially during the first stages of the life cycle, allows river bars colonization within the windows of opportunity occurring among floods.

[1] The diameter at breast height (DBH) is a standard indication of tree size and is conventionally measured at 1.4 m from the ground.

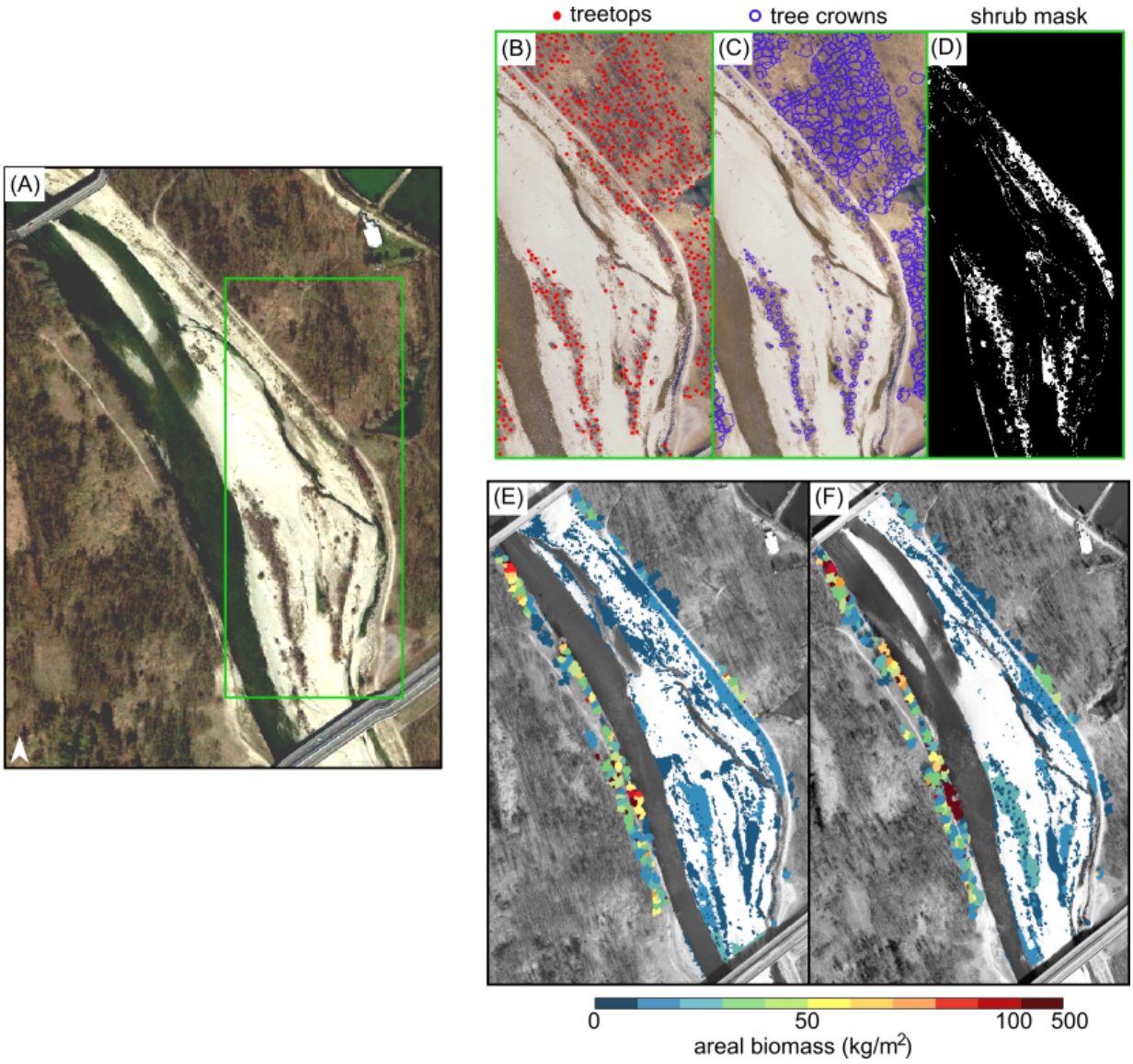

Figure 2. For a subset of the study site (A), the procedure begins with treetop detection (B) and crown segmentation (B). Later, it produces a binary mask representing shrubs (C) and computes the tree and shrub biomass. An example of the areal biomass map for 2019 (E) and 2021 (F).

4. DISCUSSION

Our analysis revealed that the goodness of the vegetation mapping is partially related to the intrinsic features of the investigated plant species and its age and that these features should drive the choice of the most suitable inventory method.

The individual tree detection algorithm works better for plants having ligneous stems, preferably with moderate stem density. Therefore, its application should cover areas with mature vegetation. The literature offers allometric relationships for adult trees to derive plant diameter from the LiDAR-derived heights. Hence, biomass estimation is straightforward if assuming the tree geometry consistent with a cylinder having the same diameter as the DBH. We also associated tree geometry with Baptist (2005) equation in eco-morphodynamic and hydraulic numerical models to compute the related roughness. Baptist (2005) approximates plants as cylinders of given rigidity, and this assumption easily holds for mature trees.

For younger trees and bushes, comparing field-measured geometrical features with the values obtained by LiDAR data demonstrated the feasibility of the geometrical reconstruction of vegetation from point clouds. In this case, volume to biomass conversion relies on bulk densities that must be estimated in the field through a procedure that recalls the slicing carried out by the underlying algorithm. Shrub-related roughness estimation is likely better described by laws other than Baptist (2005), such as those considering the plant leaf area index (LAI) (e.g., Box et al., 2021).

In the present version, the procedure estimates all the non-submerged aboveground biomass, excluding grass species, and it is customizable. For instance, it might be updated to deal with multispectral imagery and measure vegetation biomass based on particular spectral indices, such as the Normalized Difference Vegetation Index (NDVI). Whereas grass biomass might be overlooked for large-scale carbon budgets, the suggested update should be considered for generating roughness maps.

The range of applicability of the proposed procedure in this current version is from boreal to temperate climates, likely requiring modifications otherwise. For instance, biomass estimation for equatorial and tropical forests might rely on geometrical reconstruction only regardless of the vegetation age to overcome the difficulties of detecting individual plants in multilayered, fast-growing, and interlacing vegetation.

The potential of ALS surveys in mapping and modeling the vegetation is high, and future research can address the existing shortcomings. The plant height under-estimation typical of ALS can be compensated by calibrating models based on field measurement. For instance, we regressed a volume correction factor. Field-based calibration of LiDAR-derived metrics is common in forestry (Yu et al., 2010) and enables us to implement vegetation analysis over extended areas with little effort. This activity would not have been feasible with field surveys only, but it does need to be grounded on field data. Therefore, we consider remote sensing complementary and not a replacement for field activities.

5. CONCLUSIONS

Eco-morphodynamic models require information about plant geometry, spatial arrangement, and biomass to compute realistic roughness and set routines for vegetation dynamics and their influence on the morphological evolution of river floodplains. This work shortly describes the recent efforts made to address the use of remote sensing data to provide this information for continuous and extended domains. It focuses on Light Detection And Ranging (LiDAR) since airborne laser scanner LiDAR technology offers a good compromise between spatial resolution and areal coverage, and the availability of its datasets is increasing fast. Although the presented techniques are still at their early stage, they offer a starting point to merge forestry and hydraulic knowledge to study riparian corridors. By explaining their underlying workflows and highlighting their strengths and weaknesses, we provided an overall picture of using point clouds as input for eco-morphodynamic studies. Finally, we gave some insights about the future challenges to address the improvement of the presented methods while integrating different data sources and processing techniques.

6. ACKNOWLEDGEMENTS

The authors are grateful to the GMG - Geohazard Monitoring Group of CNR - IRPI (Italy) that produced and provided the airborne laser scanner data used in our examples.

7. REFERENCES

Baptist, M.J., 2005. Modelling floodplain biogeomorphology. Ph.D. thesis, Delft University of Technology.

Belcore, E., and Latella, M. (under review). Riparian ecosystems mapping at fine-scale: a density approach based on multi-temporal UAV photogrammetric point clouds. *Remote Sensing in Ecology and Conservation*.

Box, W., Järvelä, J., and Västilä, K. (2021). Flow resistance of floodplain vegetation mixtures for modelling river flows. *Journal of Hydrology*, 601, 126593.

Carbonneau, P., and Piégay, H. (Eds.). (2012). *Fluvial remote sensing for science and management*. John Wiley & Sons.

Cartisano, R., Mattioli, W., Corona, P., Mugnozza, G. S., Sabatti, M., Ferrari, B., ... and Giuliarelli, D. (2013). Assessing and mapping biomass potential productivity from poplar-dominated riparian forests: A case study. *Biomass and bioenergy*, 54, 293-302.

Duncanson, L., and Dubayah, R. (2018). Monitoring individual tree-based change with airborne lidar. *Ecology and evolution*, 8 (10), 5079-5089.

Huylenbroeck, L., Laslier, M., Dufour, S., Georges, B., Lejeune, P., and Michez, A. (2020). Using remote sensing to characterize riparian vegetation: A review of available tools and perspectives for managers. *Journal of environmental management*, 267, 110652.

Huylenbroeck, L., Latte, N., Lejeune, P., Georges, B., Claessens, H., and Michez, A. (2021). What Factors Shape Spatial Distribution of Biomass in Riparian Forests? Insights from a LiDAR Survey over a Large Area. *Forests*, 12 (3), 371.

Järvelä, J. (2004). Determination of flow resistance caused by non-submerged woody vegetation. *International Journal of River Basin Management*, 2 (1), 61–70.

Kleinhans, M.G., de Vries, B., Braat, L., and van Oorschot, M. (2018). Living landscapes: Muddy and vegetated floodplain effects on fluvial pattern in an incised river. *Earth surface processes and landforms*, 43 (14), 2948-2963.

Latella, M., Bertagni, M.B., Vezza, P., and Camporeale, C. (2020). An integrated methodology to study riparian vegetation dynamics: From field data to impact modeling. *Journal of Advances in Modeling Earth Systems*, 12 (8), e2020MS002094.

Latella, M., Sola, F., and Camporeale, C. (2021). A Density-Based Algorithm for the Detection of Individual Trees from LiDAR Data. *Remote Sensing*, 13 (2), 322.

Muneepeerakul, R., Rinaldo, A., & Rodriguez-Iturbe, I. (2007). Effects of river flow scaling properties on riparian width and vegetation biomass. *Water resources research*, 43 (12).

van Oorschot, M., Kleinhans, M., Geerling, G., and Middelkoop, H. (2016). Distinct patterns of interaction between vegetation and morphodynamics. *Earth Surface Processes and Landforms*, 41 (6), 791-808.

Perona, P., Molnar, P., Savina, M., & Burlando, P. (2009). An observation-based stochastic model for sediment and vegetation dynamics in the floodplain of an alpine braided river. *Water Resources Research*, 45 (9).

Piégay, H., Arnaud, F., Belletti, B., Bertrand, M., Bizzi, S., Carbonneau, P., ... and Slater, L. (2020). Remotely sensed rivers in the Anthropocene: State of the art and prospects. *Earth Surface Processes and Landforms*, 45 (1), 157-188.

Rahman, M.Z.A., and Gorte, B. (2008). Individual tree detection based on densities of high points of high resolution airborne LiDAR. *GEOBIA*, 350-355.

Straatsma, M.W., and Baptist, M.J. (2008). Floodplain roughness parameterization using airborne laser scanning and spectral remote sensing. *Remote Sensing of Environment*, 112 (3), 1062-1080.

Vesipa, R., Camporeale, C., and Ridolfi, L. (2017). Effect of river flow fluctuations on riparian vegetation dynamics: Processes and models. *Advances in Water Resources,* 110, 29-50.

Yu, X., Hyyppä, J., Holopainen, M., & Vastaranta, M. (2010). Comparison of area-based and individual tree-based methods for predicting plot-level forest attributes. *Remote Sensing*, 2 (6), 1481-1495.